Tunable graded cavity resonator integrated grating filters

Sylvain Augé, Antoine Monmayrant, Sylvain Pelloquin, Jean-Baptiste Doucet, Olivier Gauthier-Lafaye

Tunable Graded Cavity Resonator Integrated Grating Filters

Published in Opt. Express 25, 12415-12420 (2017)
DOI : 10.1364/OE.25.012415

S. Augé, A. Monmayrant, S. Pelloquin, J.B. Doucet, and O. Gauthier-Lafaye

Abstract

We demonstrated Graded Cavity Resonator Integrated Grating Filters (G-CRIGFs) that are narrowband spectral reflectors, spectrally tunable over more than 40 nm around 850 nm using a spatial gradient. A simple analytical model is introduced and validated experimentally to determine spectral performance of G-CRIGFs from the spectral properties of a standard Cavity Resonator Integrated Grating Filter (CRIGF).

1 Introduction

Cavity Resonator Integrated Grating Filters (CRIGFs) are spectrally narrow and efficient reflective filters[1, 2] derived from the more widespread guided modes resonant filters (GMRFs)[3]. GMRFs and CRIGFs both rely on grating coupler (GC) to couple free-space waves to a guided mode inside a planar waveguide and exhibit Fano spectral resonance when Bragg coupling conditions are met. One striking difference is that GMRFs couple to a propagating guided-mode below a large area GC, while CRIGFs couple to a standing-wave guided mode[4, 5], localized under a short GC by two side Distributed Bragg Reflectors (DBRs) (see Fig. 1). This induces two key differences: first, GMRFs have extremely low angular tolerance whereas CRIGFs show unprecedented angular tolerance[6] and second, the position of the spectral resonance of a GMRF can be tuned with the angle of incidence while that of a CRIGF is unaffected.

In fact, the shape of the spectral resonance of a CRIGF cannot be tuned by varying the conditions of incidence. The only modification is the overall amplitude of the resonance that is maximised when the overlap between the incident beam and the standing guided mode is maximised[6].

In [7], a small tuning range of the resonance was achieved by shifting, at the design stage, the position of the GC between the DBRs. However, the spectral width, shape and peak reflectivity varied greatly with the tuning. Discrete spectral tuning between identical CRIGFs fabricated above a wedged buffer

layer and a wide-band reflector is also reported in [8]. For GMRFs, and other periodic devices, introducing a spatial gradient of periodicity is a well-known approach to induce spatial tuning of the optical properties[9]. However, for CRIGFs this approach may compromise the stability of the Fabry-Pérot cavity that localizes the mode, as it breaks the lateral invariance of the structure. It has even been shown that using more stable cavities with curved DBRs increases the CRIGF performances[10]. Since CRIGFs are finite, periodic resonant structures, full 3D modelling of their optical properties is extremely complex[11] and almost impossible for a continuously graded structures.

In this paper, we experimentally investigate spatially graded CRIGFs (G-CRIGFs) and demonstrate large spectral tuning of the resonant wavelength along the gradient of periodicity of the device. A simple analytical rule to determine G-CRIGF spectral properties from that of normal CRIGF is proposed and validated experimentally using a systematic study of the optical properties with varying strengths of the gradient.

2 Samples fabrication and characterization

We based our G-CRIGF design on a standard CRIGF design depicted on Fig. 1(a). A CRIGF is composed of a central grating of period Λ (grating coupler (GC) section) surrounded by 2 DBRs (gratings of period $\Lambda/2$). Two phase shift sections (PS), of length $\phi \times \Lambda$, ensure spectral matching of the GC with the Fabry-Pérot cavity formed by the two DBRs. The whole structure is parametrically defined by the period Λ of the GC. The GC section is 21Λ-long, with a 25% filling factor (ratio of grooves width over Λ). The DBRs are 300Λ-long, with a 50% filling factor. The phase-shifts (PS) are $\phi\Lambda = 1.125\Lambda$ long. Standard CRIGFs form a planar cavity along the x-direction and is considered invariant along the y-direction. We designed our G-CRIGF with a gradient in Λ along the y-direction (linear homotetical growth of Λ with y).

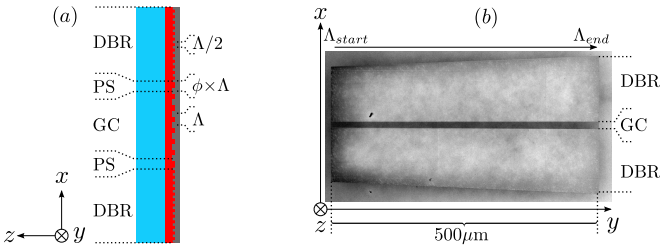

Figure 1: (a) CRIGF schematic, with glass substrate (blue), etched Si_3N_4 waveguide (red) and resist capping layer (grey). (b) optical microscope view of a fabricated G-CRIGF.

Nine G-CRIGFs, with increasing gradient strength and labelled g_1 to g_9 were fabricated on the same glass substrate (AF-32 from Schott) using a pla-

nar, parallel, fabrication process. All fabricated G-CRIGFs are 500-μm-long and start with a period $\Lambda_{start} = 510\,\text{nm}$ (see Fig. 1(b)). They exhibit a linear gradient along y to end with $\Lambda_{end} = 510$ (reference, un-graded), 515, 520, 525, 530, 540, 550, 560 and 610 nm. The fabrication process is the following. A 170-nm-thick waveguide of Si_3N_4 (optical index of 1.94 at 850 nm) is deposited by ICP-PECVD. G-CRIGF patterns are then defined on the sample by soft-mold UV-nanoimprint lithography, and etched 60-nm-deep in the waveguide. The etch depth was confirmed by AFM measurements. After cleaning, an home-made resist was used as a planarization layer, resulting in a $\simeq$70-nm-thick capping layer (optical index of 1.5 at 850 nm). Figure 1 shows a sketch of the G-CRIGF geometry and the axes notations we used in this paper. Mechanical profilometer measurements show that the capping resist thickness is constant over a large fraction of each G-CRIGF, and shows a progressive thickening at the edges of each device.

After fabrication, the G-CRIGFs were characterized using a dedicated experimental setup. A fibre-coupled swept-laser source (BS-840-1-HP from Superlum with an 0.06 nm spectral width tunable within [820:870] nm) is collimated with a 50-mm-focal-length lens. After going through a $\lambda/4$ waveplate for polarization control and a 50/50 beamsplitter, the beam is focused on the sample using a combination of 2 lenses ($f_1 = 75\,\text{mm}$ and $f_2 = 400\,\text{mm}$). The resulting beam waist is measured to be $\simeq 10\,\mu$m in the sample plane. Backreflected light is collected at the output of the beamsplitter and detected using an amplified photodiode. For calibration, a gold mirror was used in place of the sample.

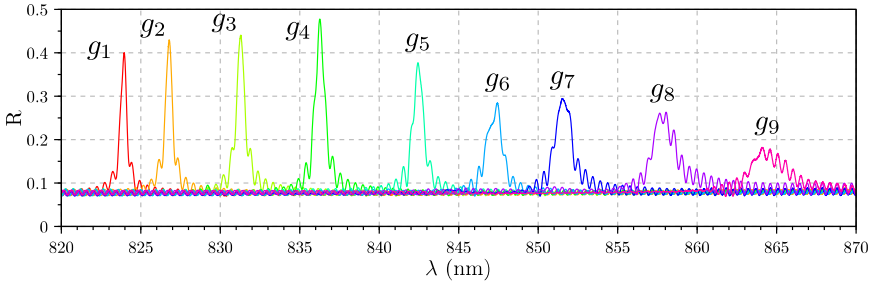

Figure 2: Typical reflectivity spectra of the 9 fabricated G-CRIGFs.

Figure 2 shows typical reflectivity spectra measured on the 9 fabricated G-CRIGFs. Narrow-band peaks (0.6 nm FWHM) are achieved for the quasi-constant G-CRIGFs g_1 and g_2. Peak reflectivity around 0.4-0.5 for such a linewidth is typical with our fabrication technique and seems to be limited by losses in the DBRs. For G-CRIGFs with stronger gradients, the peaks gets gradually broader and smaller.

For each G-CRIGF, the reflectivity was measured along the y-direction of the sample, every 10 μm. Figure 3 shows the spectral maps obtained for each sample (black stripes indicate regions where either the device was not functional

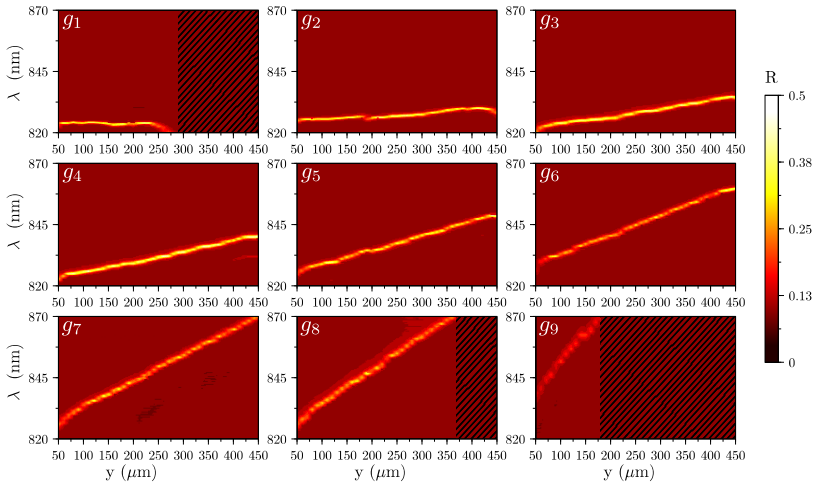

Figure 3: Spectral reflectivity maps along y for the 9 fabricated G-CRIGFs (in the stripped regions the device was either not functional or out of the tuning range of our source).

due to fabrication imperfections or the reflectivity peak was out of the tuning range of our source). As seen, the wavelength of reflection peak shifts when the probe beam is moved along y. These maps clearly show the tuning of the resonance with the G-CRIGF period, demonstrating the potential of this approach to design tunable CRIGFs. Depending on the sample, the tuning range is limited either by the G-CRIGF extension or the tuning range of our source. The maximum demonstrated spectral tuning range is above 40 nm with G-CRIGF g_8.

3 Results analysis and discussion

These results allow us to analyse the impact of the G-CRIGF gradient on its spectral response. We first focus on the tuning properties of the peak wavelength. In a second part, we quantify the impact of the G-CRIGF gradient strength on the reflectivity and spectral width.

3.1 Resonant wavelength tuning

It has already been shown that CRIGF resonances are governed by the resonant excitation of the guided mode by the GC. As for GMRFs, the resonant wavelength λ_r is such that :

$$\lambda_r = n_{eff}\Lambda \tag{1}$$

where n_{eff} is the effective index of the guided mode and Λ is the GC period. Since n_{eff} is fixed and we are using a linear variation of Λ along the y-direction, we expect a linear variation of λ_r with y. Figure 4 (a) shows the evolution of the reflection peak wavelength λ_r when the probe beam is moved inside a G-CRIGF along y. As the thickness of the resist capping layer is uniform only in the central part of each device, the refractive index of the guided mode n_{eff} varies on the edges, biasing the determination of the gradient. We thus only keep measurements made inside the uniform regions (solid points) to estimate the gradient using a linear fit (solid lines), ignoring measurements made on the edges of each device (crosses). As seen from the good alignement of the experimental data points with the linear fits, the variation of λ_r is indeed linear with the position y for each device.

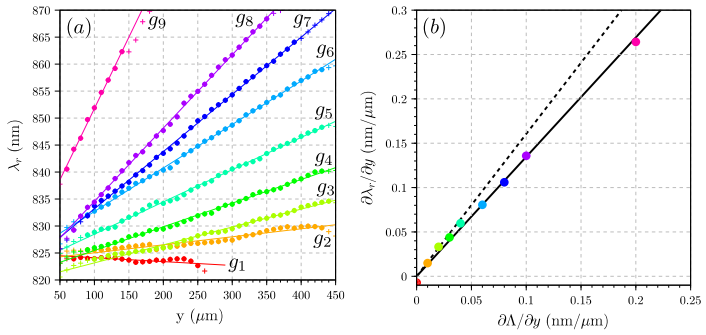

Figure 4: (a) Experimental reflectivity peak wavelength versus y-position on the G-CRIGF. Solid lines are linear fits based on the solid color dots (cross points were ignored). (b) Peak wavelength gradient versus period gradient. Dots correspond to the linear fits on the left figure. Dashed line is the theoretical curve using the effective index of the waveguide (eq. 1). Full line is the theoretical curve taking waveguide dispersion into account according to eq. 2.

On Figure 4 (b), we plot the gradient of the peak wavelength $\partial\lambda_r/\partial y$ as a function of the gradient of the GC period $\partial\Lambda/\partial y$. Looking at eq.1, one might expect a linear relation with a slope $n_{eff} \simeq 1.61$ (dashed line on Fig. 4 (b)). As seen, this relation over-estimates the gradient of the peak wavelength. To explain this, we have to look more closely at eq.1 and derive a proper differentiation. Indeed, n_{eff} is not a constant, but a function of λ_r, and thus indirectly depends on y. Differentiating eq.1 with respect to y thus leads to:

$$\frac{\partial\lambda_r}{\partial y} = n_{sg} \times \frac{\partial\Lambda}{\partial y} \quad \text{with} \quad n_{sg} = n_{eff} \times \left(1 - \frac{\lambda_r}{n_{eff}} . \frac{dn_{eff}}{d\lambda}\right)^{-1} \tag{2}$$

Similarly to the expression of the free spectral range (FSR) of a laser diode, where the group index (and not the effective index) has to be taken into account, here we have some kind of *spatial group index* (n_{sg}) instead of *spectral*

group index. Extracting the effective index of the guided mode and its spectral dependence from the experimental relationship between λ_r and Λ_{GC} leads to a value of $n_{sg} = 1.35$ (solid line in Fig. 4(b)), in good agreement with the value of 1.37 calculated using the nominal layers thicknesses and taking into account the index dispersion in our materials.

3.2 Reflectivity and spectral width

In this section, we investigate the consequences of the gradient on the GC period Λ on the peak reflectivity and spectral width of the G-CRIGF resonance. Figure 5 shows the evolution of the reflectivity and spectral width (Full Width at Half Maximum FWHM) of the fabricated G-CRIGFs versus the gradient of the GC period, expressed in nm/μm. Each color dot represents the median of the measured values (peak reflectivity or FWHM) along each G-CRIGF, the black brackets representing the standard deviation. As seen, and as expected, the maximum reflectivity decreases and the FWHM increases with increasing values of the gradient of the GC period.

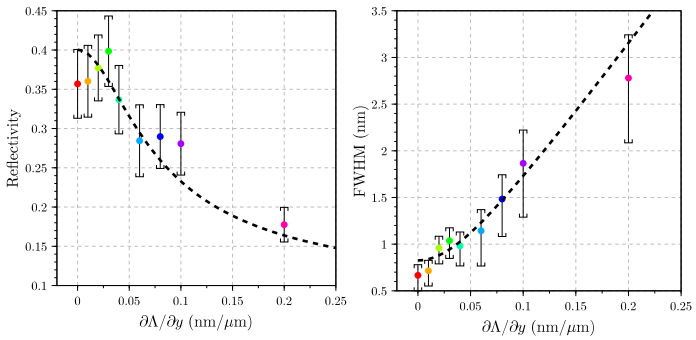

Figure 5: Evolution of reflectivity and spectral width of the resonance versus gradient of the period. Solid color dots correspond to the median of experimental values, black brackets giving the standard deviation. Dashed lines correspond to best fit using eq. 5.

For further analysis, we build a simple 1D model of the G-CRIF reflectivity. We consider a Gaussian probe beam with an intensity expressed as:

$$I(y) = I_0 \exp\left[-2\left(\frac{y - y_0}{w_0}\right)^2\right] \tag{3}$$

where w_0 is the beam waist and y_0 the center of the Gaussian. We assume that the spectral reflectivity of a CRIGF can be modelled as a Gaussian spectrum:

$$R = R_b + R_0 \exp\left[-2\left(\frac{\lambda - \lambda_r}{\Delta\lambda}\right)^2\right] \tag{4}$$

where R_b is the baseline reflectivity, R_0 is the resonance amplitude and $\Delta\lambda$ its spectral width. The resonant wavelength λ_r varies linearly along y as already discussed. We then assume that the overall reflectivity of the G-CRIGF $R_g(\lambda)$ is the sum of the local reflectivities weighted by the local beam intensity. Straightforward calculations leads to the following result:

$$R_g(\lambda)\frac{\int I(y)R(y,\lambda)dy}{\int I(y)dy} = R_b + R_0 \frac{\Delta\lambda}{\left(\Delta\lambda^2 + \left(w_0\frac{\partial\lambda_r}{\partial y}\right)^2\right)^{1/2}} \exp\left[\frac{-2\left(\lambda-\lambda_r\right)^2}{\Delta\lambda^2 + \left(w_0\frac{\partial\lambda_r}{\partial y}\right)^2}\right] \tag{5}$$

where we have defined the resonant wavelength of the G-CRIGF as $\lambda_r = \lambda(y_0)$. Taking into account a measured baseline reflectivity of $R_b = 0.08$ (see Fig. 3), we fitted our experimental measurements with this formula (dashed lines in Fig. 5), resulting in a beam waist of $w_0 = 9.6\,\mu$m, a resonance amplitude $R_0 = 0.3$ and a spectral width $\Delta\lambda = 0.7\,$nm. As seen, this simple model accurately described the observed experimental trend.

From the denominators in eq. 5, we observe two possible regimes depending on the waist w_0, the spectral width $\Delta\lambda$ and the gradient of period $\partial\lambda_r/\partial y$. For small waists, small gradients and large spectral widths ($\Delta\lambda \gg w_0\partial\lambda_r/\partial y$), spectral width and peak reflectivity of the G-CRIGF are similar to that of the equivalent CRIGF. On the contrary, when the gradient over the extension of the waist cannot be neglected as compared to the initial spectral width, the spectral width increases and the peak reflectivity decreases as compared to the equivalent CRIGF.

4 Conclusion

We have demonstrated graded CRIGFs (G-CRIGFs) with continuous tuning of the reflectivity peak (FWHM of $\simeq 1.8\,$nm) over a wide wavelength range of 40 nm around 850 nm. We have shown that the presence of a spatial gradient along the transverse direction in the CRIGF cavity does not necessarily degrade the spectral performance. This indicates that the formation of a localized standing wave inside the G-CRIGF can be achieved despite the presence of the gradient. The optical performance of a G-CRIGF can be directly deduced from the performance of an equivalent standard CRIGF using simple analytical model of weighted averaging of the local reflectivities. This work opens the way to designing optimized G-CRIGFs where the gradient amplitude is balanced to achieve high tuning rate while maintaining a narrow enough spectral width for a given application. Such optimizing will be particularly useful for applications such as tunable external cavity laser diodes.

Funding

S. Augé acknowledges financial support from DGA and Centre National d'Etudes Spatiales (CNES) PhD grants under the supervision of P. Adam and B. Faure. We acknowledge financial support from CNES under grant n° 130251 and from Agence Nationale de la Recherche under grant ANR14-ASTR-0024-01.

Acknowledgments

Authors thankfully acknowledge the LAAS clean room team for technical support and technological expertise provided within the french RENATECH framework.

References

[1] K. Kintaka, T. Majima, J. Inoue, K. Hatanaka, J. Nishii, and S. Ura, "Cavity-resonator-integrated guided-mode resonance filter for aperture miniaturization," Opt. Express **20**, 1444–1449 (2012).

[2] S. Ura, J. Inoue, K. Kintaka, and Y. Awatsuji, "Proposal of small-aperture guided-mode resonance filter," in "2011 13th International Conference on Transparent Optical Networks," (2011), pp. 1–4.

[3] S. Tibuleac and R. Magnusson, "Reflection and transmission guided-mode resonance filters," JOSA A **14**, 1617–1626 (1997).

[4] R. Laberdesque, O. Gauthier-Lafaye, H. Camon, A. Monmayrant, M. Petit, O. Demichel, and B. Cluzel, "High-order modes in cavity-resonator-integrated guided-mode resonance filters (crigfs)," J. Opt. Soc. Am. A **32**, 1973–1981 (2015).

[5] N. Rassem, A.-L. Fehrembach, and E. Popov, "Waveguide mode in the box with an extraordinary flat dispersion curve," J. Opt. Soc. Am. A **32**, 420–430 (2015).

[6] X. Buet, E. Daran, D. Belharet, F. Lozes-Dupuy, A. Monmayrant, and O. Gauthier-Lafaye, "High angular tolerance and reflectivity with narrow bandwidth cavity-resonator-integrated guided-mode resonance filter," Optics express **20**, 9322–9327 (2012).

[7] K. Kintaka, K. Asai, K. Yamada, J. Inoue, and S. Ura, "Grating-Position-Shifted Cavity-Resonator- Integrated Guided-Mode Resonance Filter," IEEE Photonics Technology Letters **29**, 201–204 (2017).

[8] K. Yanagida, K. Mori, M. Nakata, J. Inoue, S. Ura, and K. Kintaka, "Characterization of CRIGF integrated on DBR substrate," in "CPMT Symposium Japan (ICSJ), 2016 IEEE," (IEEE, 2016), pp. 173–176.

[9] P. Srinivasan, M. K. Poutous, Z. A. Roth, Y. O. Yilmaz, R. C. Rumpf, and E. G. Johnson, "Spatial and spectral beam shaping with space-variant guided mode resonance filters," Optics express **17**, 20365–20375 (2009).

[10] K. Hatanaka, T. Majima, K. Kintaka, J. Inoue, K. Nishio, Y. Awatsuji, and S. Ura, "Cavity-resonator-integrated guided-mode resonance filter consisting of curved gratings," Electronics Letters **48**, 717–718 (2012).

[11] P. C. Chaumet, G. Demésy, O. Gauthier-Lafaye, A. Sentenac, E. Popov, and A.-L. Fehrembach, "Electromagnetic modeling of large subwavelength-patterned highly resonant structures," Opt. Lett. **41**, 2358–2361 (2016).